JP5J.3 BOW ECHOES DURING BAMEX: ASSESSING TRANSITIONS IN SURFACE WIND DAMAGE USING WSR-88D DATA

Michael C. Kruk *
Midwestern Regional Climate Center, Champaign, Illinois

Robert M. Rauber, Greg M. McFarquhar, Brian F. Jewett
University of Illinois, Champaign, Illinois

Robert J. Trapp
Purdue University, Lafayette, Indiana

1. INTRODUCTION

The Bow Echo and Mesoscale Convective Vortex Experiment (BAMEX) was conducted from 20 May to 6 July 2003 to study the life cycle of Mesoscale Convective Systems (MCSs) and associated bow echoes and mesoscale convective vortices (Davis et al. 2004). Of the missions that were investigated during BAMEX, nine produced bow echo MCSs with trailing stratiform precipitation, one produced a bow echo with leading stratiform precipitation, ten focused on mesoscale convective vortices (MCVs), and three were frontal squall lines that exhibited both parallel and trailing stratiform precipitation. The analysis in this study was performed on those events whose convection began as initial cells, developed into a quasi-linear system, and finally into a bow echo with well developed trailing stratiform precipitation. Ten events met these criteria and are summarized in Table 1.

This investigation considers whether the type of wind-produced damage in bow echoes demonstrates a temporal transition during the MCS life cycle. Specifically, it is examined whether the type of wind-produced damage early in bow echo producing MCSs transitions from tornadoes and downbursts early in the MCS lifetime to predominantly straight-line winds once rear inflow has developed. The widespread availability of Weather Surveillance Radar-1988 Doppler (WSR-88D) level II and level III radar data, in conjunction with BAMEX damage surveys (Atkins et al. 2005; Wheatley et al. 2005) and concomitant public damage reports, provides an opportunity for a systematic assessment of the radial velocity data at each damage report and survey location. The radar radial velocity data was scrutinized at each damage report and survey location to classify a radar-determined source of damage. Three types of radar signatures were examined: straight-line winds from rear inflow as well as rotational and downburst couplets.

2. DATA & METHODOLOGY

All ten Intensive Operations Periods (IOPs) took place over areas of the United States that are well represented by the aerial coverage of at least one WSR-88D radar. WSR-88D level II and level III radar data provided a means through which radial velocities can be compared against all wind damage reports for each IOP. Additionally, the availability of damage surveys performed during BAMEX provides well-documented ground-truth descriptions that compliment the damage reports. Often times these damage surveys included detailed areas of downburst, straight-line wind, and tornado damage (Atkins et al. 2005; Wheatley et al. 2005).

Damage reports for all ten IOPs used in this study were obtained from the Storm Prediction Center's Severe Thunderstorm Database (Schaefer 1999). Duplicate reports (those with the same latitude and longitude) were deleted. Since we were only interested in wind damage, all hail damage reports were omitted.

BAMEX damage survey results (Atkins 2005; Wheatley 2005) were obtained for IOPs 1, 2, 3, 7, 12, 17, 18, and the 10 June 2003 bow echo that passed over the BAMEX Operations Center. For each surveyed location, the location and nature of the damage (e.g., straight-line wind, downburst, etc.) were added to the damage reports.

For the ten BAMEX IOPs used in this study, 260 damage reports were available. At each damage report location, the time of the report was associated with a time on radar. Many of the damage report times were inconsistent with the location of the storm on radar. For example, during IOP 4 (2-3 June 2003), the time on a few damage reports was approximately one hour before the storm system arrived at the damage location. Additionally, there were instances where the time of the damage report was two to four hours after the storm system had passed.

For this study, it was assumed that the time of the actual damage occurrence coincided with the time at which the storm system passed directly over the location of the reported damage. This method was also used to associate a time on radar with each location where damage surveys were conducted.

Couplets of inbound and outbound radial velocities were associated with rotation if the angle between the radar beam and the axis between the maximum inbound and outbound velocities within the couplet was greater than or equal to 45 degrees. An angle of 90 degrees represents pure rotation. Eighty three percent of all identified rotational couplets at the locations of the damage reports had maximum ground-relative radial velocities greater than 25 ms^{-1}, the National Weather Service's minimum wind speed required for a thunderstorm to be categorized as severe.

* *Corresponding author address*: Michael C. Kruk, Midwestern Regional Climate Center, Champaign, IL 61820; email: mkruk@sws.uiuc.edu

Although mesocyclone-scale rotation was easily identified in the radial velocity field, mesovorticies along gust front boundaries were very difficult to identify. The height of the radar beam, the resolution of the radar sample volume relative to the size of the mesovortex, and the angle of the radar beam relative to the gust front all impeded the detection of mesovortices. While shear induced vortices may have been responsible for some of the reported damage, it was difficult to ascertain where these mesovortices were located. These short-lived mesovortices along gust fronts were generally not possible to locate, and were not included in the analysis presented here.

Downbursts were identified on radar if they had distinct velocity couplets where the angle between the radar beam and the axis connecting the maximum inbound and outbound velocities within the couplet was less than 45 degrees. Sixty-seven percent of the detected downbursts at the location of the damage reports had maximum ground-relative radial velocities exceeding the severe criteria set by the National Weather Service (25 ms^{-1}).

Rear inflow was characterized in the radar radial velocity data if it had a core of maximum ground-relative wind speed that was greater than or equal to 15 ms^{-1} and exhibited a strong line-normal component directed toward the center of the squall line. Rear inflow based damage was defined as straight-line wind damage without rotational or downburst couplets. Furthermore, no differentiation was made between descending and non-descending rear inflow.

Eighty-six percent of the maximum radial velocities observed within the rear inflow at each damage point exceeded 25 ms^{-1}. In many situations, the convective line was oriented at an angle relative to the radar beam so that the total velocity of the rear inflow was not well represented by the measured radial velocity. In order to get a more representative sampling of the radial velocity within rear inflow over the damage location, an estimated total velocity was calculated. To estimate the maximum rear inflow velocity, the measured radial velocity was adjusted by the cosecant of the angle between the beam and axis normal to the orientation of the convective line. This calculation was done only when the orientation angle was greater than or equal to thirty degrees. Smaller angles resulted in estimated total velocities that were often clearly unrealistic. Over 90% of the rear inflow estimated maximum total velocities at the damage locations were greater than 25 ms^{-1} with this adjustment.

Occasionally, there were storm damage reports that occurred on the periphery of the storm complex. Generally, these reports occurred at a wide angle relative to the direction of the convective line. It appears that in these cases the outflow from the convective system spread outward from the core of the system at an angle nearly orthogonal to the direction of movement of the MCS. Many of the IOPs exhibited damage along the gust fronts at the periphery of the storm complex. These damage reports were classified as peripheral gust fronts. These peripheral gust fronts, which occurred only when rear inflow was present, accounted for 8% of the damage reports.

The radar-determined source of damage at 31% of all damage reports was indeterminable. This classification resulted when the orientation angle of the radar beam relative to the convective line was too large, the radar beam was too high, or radial velocity ambiguities existed over the damage location. The orientation angle of the radar beam to the convective line added complexity in recognizing radar radial velocity signatures.

3. DAMAGE TRANSITIONS

The radar-determined sources of damage, though different between events, exhibited some similarities with respect to the temporal evolution of most MCSs. In general, in the early portion of the storm, the damage reports were characterized by rotational or downburst couplets. As the storm systems evolved with time, the radar-determined source of damage was comparatively more attributable to rear inflow.

The results of the analysis show that many of the damage reports were point specific prior to the recognition of rear inflow on radar. Once rear inflow was identified, many of the damage reports were in the center of each county. In addition, many of these damage reports contained information such as “trees down across the county”, implying countywide damage. Fig. 1 shows the distribution of damage for all IOPs relative to the time that rear inflow aloft first became apparent in the radial velocity field. The x-axis is binned by twenty minute intervals, centered around the time t = 0 when rear inflow became evident on radar. The frequency of damage reports associated with each mode of wind damage is shown. The figure clearly shows the mode of damage transition that occurs relative to the time that the rear inflow is first identified. There is a peak in the number of radar-determined sources of damage that were attributable to rear inflow between 100 and 160 minutes after the appearance of rear inflow. Beyond this time, the number of damage reports attributable to rear inflow dramatically decreases.

Prior to the identification of rear inflow on radar, only 22% of the total number of damage reports had been received. In the early stages of development, many of the BAMEX IOPs were characterized by tornadic supercell thunderstorms. Based on radar radial velocity data, 88% of all rotational couplets were identified prior to the establishment of rear inflow. Similarly, 67% of all downburst couplets were identified prior to rear inflow detection.

Once rear inflow was identified using radar radial velocities, the radar-determined source of damage attributable to rear inflow greatly outweighed those radar-determined sources of damage that were associated with either rotational or downburst couplets. Coincidentally, the number of tree damage reports dramatically increased once rear inflow was evident on radar. Fig. 2 is a frequency diagram illustrating the nature of the damage (e.g., “trees down”, “power lines

down across town", etc.), which occurred relative to the appearance of rear inflow on radar. Approximately 83% of the damage reports that mentioned tree damage occurred after the appearance of rear inflow on radar. Seventy-five percent of the damage attributable to rear inflow occurred between one and three hours after its first identification on radar.

Based on the BAMEX damage surveys, damage reports, and the WSR-88D level II and level III radar radial velocity and reflectivity data that corresponded to each damage location, the evidence reported here strongly suggests that a temporal transition exists in the mode of the wind-produced damage in bow echo producing MCSs with trailing stratiform precipitation. Prior to the identification of rear inflow aloft on radar, the radar-determined source of damage was characterized by a combination of rotational and downburst couplets. As the storm systems matured and rear inflow became established, the radar-determined sources of wind damage were almost entirely associated with rear inflow and gust fronts at the periphery of the system.

4. REFERENCES

Atkins, N.T., C.S. Bouchard, R.W. Przybylinski, R.J. Trapp, and G. Schmocker, 2005: Damaging surface wind mechanisms within the 10 June 2003 Saint Louis bow echo during BAMEX. *Mon. Wea. Rev*., (in press).

Davis, C. A., N. Atkins, D. Bartels, L. Bosart, M. Conglio, G. Bryan, W. Cotton, D. Dowell, B. Jewett, R. Johns, D. Jorgensen, J. Knievel, K. Knupp, W-C. Lee, G. McFarquhar, J. Moore, R. Przybylinski, R. Rauber, B. Smull, R. Trapp, S. Trier, R. Wakimoto, M. Weisman, and C. Ziegler, 2004: The Bow Echo and MCV Experiment. *Bull. Amer. Meteor. Soc.*, **85**, 1075-1091.

Schaefer, J.T., and R. Edwards, 1999: The SPC tornado/severe thunderstorm database. Preprints, *11th Conf. Applied Climatology*, Dallas, TX, Amer. Meteor. Soc., 603-606.

Wheatley, D.M., R.J. Trapp, and N.T. Atkins, 2005: Radar and damage analysis of bow echoes observed during BAMEX. *Mon. Wea. Rev*. (in press).

Mission	Date	Location
IOP 2	28-29 May 2003	Illinois / Indiana
IOP 4	2-3 June 2003	Kansas / Arkansas / Mississippi
IOP 7	9-10 June 2003	Nebraska / Iowa / Missouri / Kentucky / Tennessee
MAA Bow Echo	10 June 2003	Missouri / Illinois
IOP 9	20-21 June 2003	Nebraska
IOP 12	24 June 2003	Nebraska / Iowa
IOP 14	29 June 2003	Kansas
IOP 16	2-3 July 2003	Minnesota
IOP 17	4-5 July 2003	Indiana / Ohio
IOP 18	5-6 July 2003	Nebraska / Iowa

Table 1. A summary of the locations and dates of the missions examined.

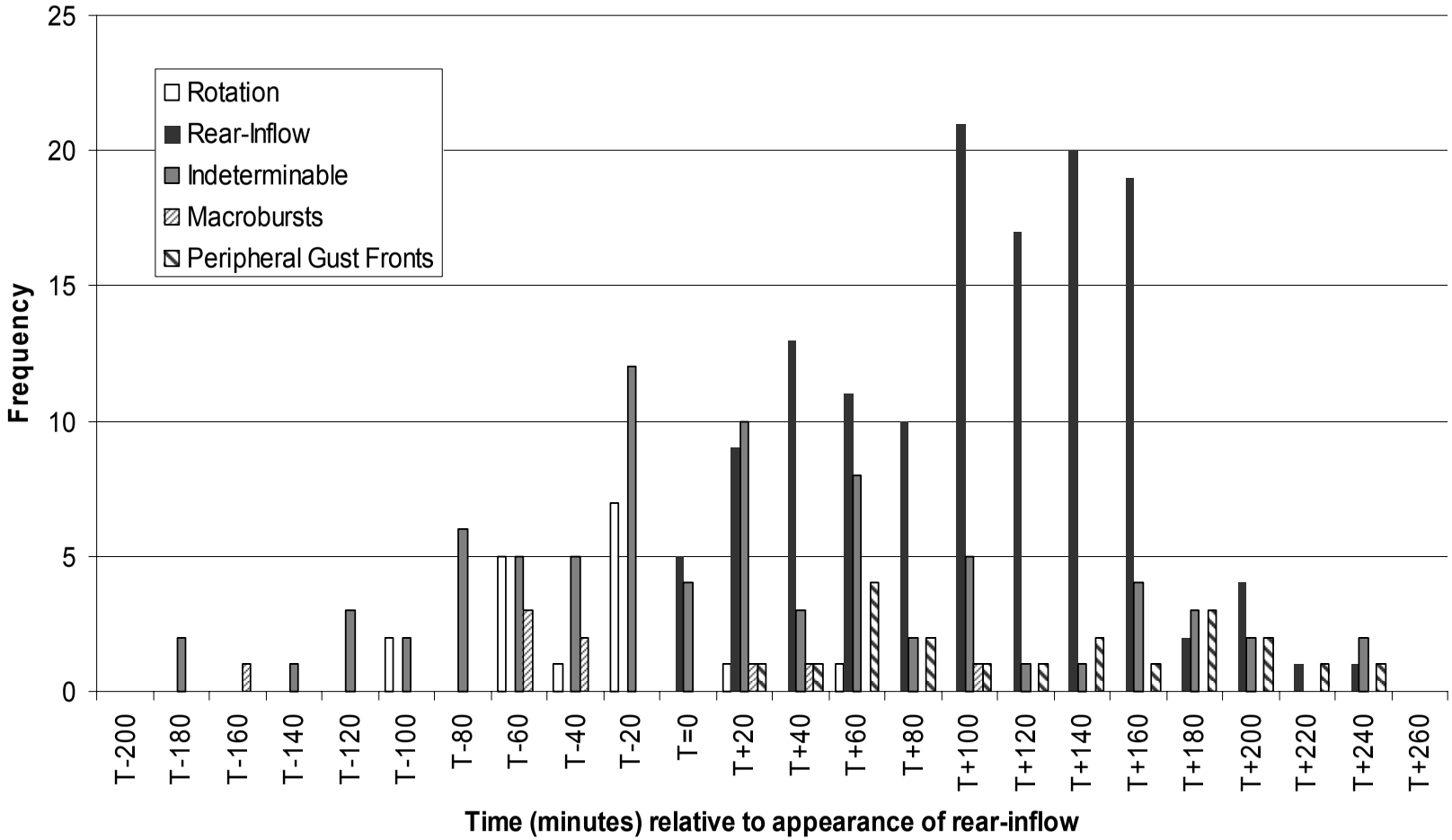

Fig. 1. Histogram showing the radar signature distribution by time relative to the appearance of the rear-inflow jet. Note the peak in rear-inflow damage after 100 minutes.

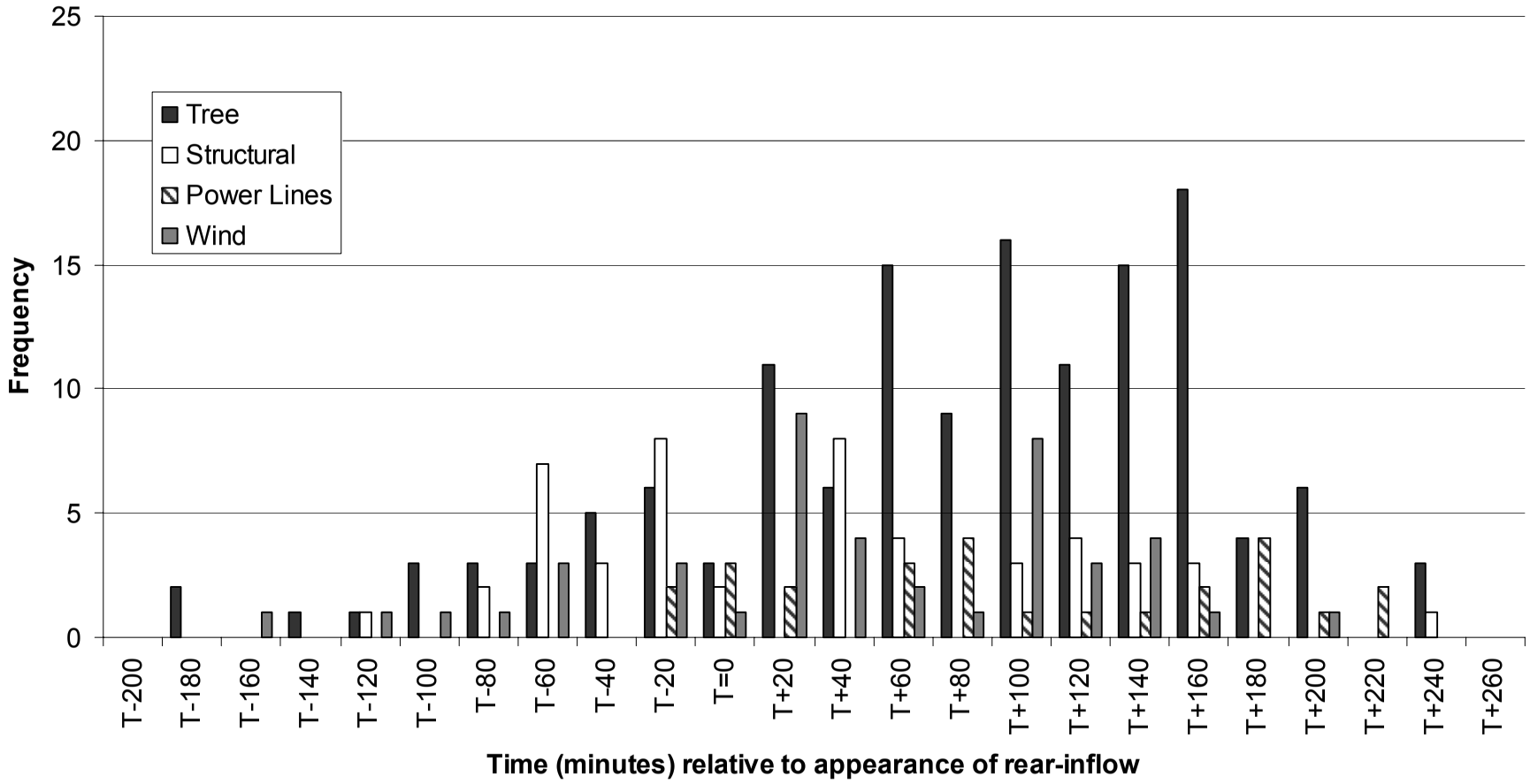

Fig. 2. A histogram showing the distribution of the reported damage relative to the recognition of rear inflow on radar.